ELSEVIER

Journal of Molecular Catalysis B: Enzymatic 11 (2001) 841–850

JOURNAL OF MOLECULAR CATALYSIS B: ENZYMATIC

www.elsevier.com/locate/molcatb

Modeling the performance of immobilized α-chymotrypsin catalyzed peptide synthesis in acetonitrile medium

Raúl J. Barros [a,b,*], Ernst Wehtje [a], Patrick Adlercreutz [a]

[a] *Department of Biotechnology, Center for Chemistry and Chemical Engineering, Lund University, P.O. Box 124, S-22100 Lund, Sweden*
[b] *Unit for Agrarian Science and Technology, University of Algarve, Campus de Gambelas, P-8000-810 Faro, Portugal*

Abstract

A model was developed which describes simultaneous reaction and internal diffusion for kinetically controlled, immobilized α-chymotrypsin-catalyzed, oligopeptide synthesis in acetonitrile medium. The model combines the equations that describe the intrinsic kinetics of four different reactions and the physical characteristics of three different support materials, as determined experimentally, to predict the apparent initial activity and nucleophile selectivity of the immobilized biocatalyst. The model is able to predict reasonably well the experimentally observed initial rate and nucleophile selectivity vs. enzyme loading profiles. The reduction in observed initial rate with enzyme loading when fast reactions are carried out with α-chymotrypsin immobilized on celite, and the larger influence of mass transfer limitations on the initial reaction rates than on nucleophile selectivities are correctly predicted by the numerical calculations. The model is general in terms of its application to other systems — enzymes, reactions, support materials and/or kinetic schemes — as long as the intrinsic kinetics and the characteristics of the enzyme and support material are known.

Keywords: Kinetically controlled peptide synthesis; Initial rate; Nucleophile selectivity; Internal diffusion and reaction; Numerical model

1. Introduction

In recent years, the improved understanding of the action of enzymes in organic media and their applications for synthetic purposes has led to a gradual improvement of the efficiency of use of biocatalysts in low-water systems, particularly in monophasic organic solvents [1–5]. Since enzymes are usually insoluble in these systems, unless otherwise conveniently engineered, these are heterogeneous catalytic systems. The immobilization of enzymes in porous carrier particles has proved to be a valuable technique in order to avoid suspended enzyme powder aggregation and compaction, and to confer a number of desirable characteristics to the biocatalyst particles, such as good mechanical and hydrodynamic resistance, defined particle size, good substrate and water partitioning and higher accessibility of the enzyme active sites. Immobilization also facilitates the use of the enzyme in continuous-flow systems, either in packed bed or stirred tank reactors, or the recovery of the biocatalyst at the end of batch processes and its reuse [3,6–8].

* Corresponding author. Tel.: +351-289-800-900 ext. 7391; fax: +351-289-815-927.
E-mail address: rbarros@ualg.pt (R.J. Barros).

1381-1177/01/$ - see front matter
PII: S1381-1177(00)00030-8

As with all heterogeneous catalyst systems, the performance of faster catalysts ultimately becomes limited by how fast the substrates can be transported to the active sites on the solid particles. External and internal diffusional limitations are then expected to exist in most, if not all, usefully fast heterogeneous catalytic systems. Even though they should be minimized, because they lead to a reduced efficiency of use of the biocatalyst, they should not be considered as a problem to be eliminated at all costs, but rather as a sign that the catalytic competence of the enzyme is not anymore the sole factor that limits the rate of the transformation. Under mass-transfer limiting conditions, simple manipulations of the biocatalyst particles, such as particle size reduction or choice of a more porous matrix for immobilization, have a larger beneficial effect on the transformation rate than any changes on the enzyme itself or its microenvironment.

Even though external diffusional limitations can be avoided by increased flow rates around the catalyst particles in fixed beds, or increased agitation rate in the case of stirred tanks, internal diffusional limitations are more difficult to avoid, and generally play a larger role [9–11]. The study of simultaneous diffusion and reaction is important in order to optimize the catalytic system, which is confirmed by the large number of publications dealing with description and mathematical modeling of this phenomenon [12–19]. The nonlinear nature of enzyme kinetics demands that the models developed are solved numerically and a number of computational tools are currently available for this task, so that presently it is possible to solve this problem with access to a simple personal computer with the adequate software [13,14,20].

In this work, we have built a model to describe the action of immobilized α-chymotrypsin synthesizing di- or tripeptides in acetonitrile medium under kinetic control. Under these conditions the substrates undergo the following enzyme-catalyzed reactions:

Formation of product:

$$\mathrm{AcD} + \mathrm{Nuc} \rightarrow \mathrm{Pep} + \mathrm{LG} \quad (1)$$

Hydrolysis of acyl donor:

$$\mathrm{AcD} + \mathrm{H_2O} \rightarrow \mathrm{HyP} + \mathrm{LG} \quad (2)$$

Two-substrate simultaneous diffusion and reaction were simulated. Four different combinations of substrates and three different support materials were modeled, and the effect of change of enzyme loading studied, and compared to the experimental profiles of initial reaction rate and nucleophile selectivity vs. enzyme loading previously collected [11,21].

2. Theory

2.1. Intrinsic kinetics

The estimation of the intrinsic (mass-transfer limitation free) kinetic parameters for enzymatic reactions in organic media is not a trivial task, specially with intrinsically fast reactions. The use of homogeneous systems is not a solution, because solubilization of enzymes in organic media usually involves association with other agents that can have a direct effect of enzyme kinetics. The only way is to ensure that mass-transfer effects are absent in heterogeneous systems as similar as possible to the immobilized preparations used. We have developed a system to carry out these kinetic studies by immobilizing thin layers of enzyme on nonporous glass beads, ensuring simultaneously that inactivation by the support is minimal, and that mass-transfer effects do not play a role [22].

The intrinsic initial kinetics of the dipeptide synthesis reactions was empirically observed to fit well the equations:

$$\frac{\mathrm{d}[\mathrm{Pep}]}{\mathrm{d}t} = \frac{k_{\mathrm{Synth}}[\mathrm{AcD}][\mathrm{Nuc}][E_0]}{K_{\mathrm{N}} + [\mathrm{Nuc}]} \quad (3)$$

and

$$\frac{\mathrm{d}[\mathrm{Hyp}]}{\mathrm{d}t} = \frac{k_{\mathrm{Hydr}}[\mathrm{AcD}][E_0]}{K_{\mathrm{N}} + [\mathrm{Nuc}]} \quad (4),$$

which describe the initial rates of dipeptide synthesis and acyl donor hydrolysis, respectively [22]. The nucleophile selectivity, defined as the ratio of pep-

tide synthesis to acyl donor hydrolysis, predicted by these equations will be:

$$\frac{\text{Rate}_{\text{Synth}}}{\text{Rate}_{\text{Hydr}}} = \frac{\text{d[Pep]}}{\text{d[Hyp]}} = \frac{k_{\text{Synth}}[\text{Nuc}]}{k_{\text{Hydr}}} \quad (5)$$

2.2. Estimation of bulk solution and effective diffusion coefficients

An estimation of the bulk solution diffusion coefficients at infinite dilution of the substrates in the solvent mixture (acetonitrile containing 5 vol.% water) was obtained by the method of Tyn and Calus [23]. Group contribution methods were used to estimate the molar volumes and the parachors (molar volumes multiplied by the 0.25th power of the surface tension) of the involved compounds [23]. The viscosity of the solvent mixture was estimated by the method of Teja and Rice [23]. The relevant parameters and the estimates of the bulk solution diffusion coefficients are presented in Table 1.

Considering that the pores have a diameter much larger than the dimensions of the diffusing molecules, the effective diffusion coefficients for diffusive transport inside the biocatalyst particles were calculated from the bulk solution diffusion coefficients using the expression [24]

$$D_{\text{eff}} = \frac{D_{\text{B}}\varepsilon}{\tau} \quad (6)$$

The volumetric porosity was calculated at each enzyme loading value on each support taking into account the volume occupied by the enzyme molecules on the pores of the immobilization support [25]. One enzyme molecule, with molecular mass 25,000, is estimated to occupy the volume of an ellipsoid with dimensions $51 \times 40 \times 40$ Å [26], which translates into a volume occupation by the enzyme of approximately 1.03 cm^3/g. In order to calculate the maximum amount of enzyme that can be fitted into the pores of a given support material, it was assumed that the enzyme molecules accommodate in a face-centered lattice, with a volume occupancy ratio of $2\pi/(3 \times 8^{0.5}) = 0.74$. In the case of the higher enzyme loadings on celite, not all the enzyme can fit into the pores of the support. In this case, the maximum attainable loading was assumed, and it was admitted that the activity of the remaining enzyme molecules outside the biocatalyst pores is negligible. This agrees with the experimental observation that non-immobilized enzyme is much less active than immobilized enzyme in the used medium, probably due to the formation of highly mass-transfer limited enzyme aggregates. In reality the borderline between the existence of enzyme only inside the particle pore and both inside and outside is not expected to be so rigid. It is probable that a fraction of the enzyme will always stay outside the particle pores, even if there is still space to accommodate it inside. The approximation used in the model, though, yields results that agree reasonably with the experimental observations.

In the absence of experimental data, pore tortuosity values for particles containing no enzyme were adjusted in order to get the best agreement between

Table 1
Bulk solution diffusion coefficients of the reactants in acetonitrile containing 5 vol.% water

Component	Molar volume (cm^3/mol)	Parachor ($\text{cm}^3\ \text{g}^{0.25}\ \text{s}^{-0.5}\ \text{mol}^{-1}$)	Viscosity (cP)
Solvent	48	112	0.55
Solutes	Molar volume (cm^3/mol)	Parachor ($\text{cm}^3\ \text{g}^{0.25}\ \text{s}^{-0.5}\ \text{mol}^{-1}$)	$D_{\text{B}} \times 10^5$ ($\text{cm}^2\ \text{s}^{-1}$)
BzAlaOMe	233	470	1.40
AcPheOEt	280	550	1.31
BzTyrOEt	350	690	1.18
AlaNH_2	102	214	1.94
AlaPheNH_2	273	540	1.31

model calculations and experimental data. Tortuosity was assumed to be inversely proportional to the volumetric porosity [24] when taking into account the reduction of porosity of the biocatalyst particles due to the space occupied by the enzyme molecules.

The effective diffusion coefficients thus depend not only on the physical characteristics of the support particles, but also on the enzyme loading.

2.3. Numerical resolution of the reaction–diffusion model

A number of approximations were used in order to build the model: spherical biocatalyst particles, uniform distribution of enzyme within the pores of the particles, intrinsic activity of the enzyme independent of enzyme loading and absence of interactions between the substrates and the biocatalyst particles that could lead to preferential partition were assumed. These are rough approximations to the real situation: the particles have irregular shapes, and we have observed that at low enzyme loading the activities are lowered because of inactivation of enzyme by direct contact with the support material [11]. In the absence of a reliable model that describes this last effect as a function of the support material used, we chose not to take it into account. This effect becomes negligible at high enzyme loading, where mass transfer becomes limiting, which are the conditions we hope to describe accurately with this mathematical model. We have no information about distribution of the enzyme within the support particles, but if acquired, it can easily be incorporated into the model by treating $[E_0]$, D_{Aeff} and D_{Neff} as functions of r. Water, which is a substrate for the hydrolytic side reaction, was assumed not to be subjected to mass transfer limitations, given its large excess — its concentration is around 2.8 M, vs. 20 mM for the acyl donor. Its concentration, or rather activity, was assumed to be constant, and thus no influence of water was assumed on intrinsic reaction kinetics. External mass transfer limitations were assumed to be negligible, as suggested by previous experimental results [11].

For a given biocatalyst (support material and enzyme loading defined) and a given R, the differential equations that describe the substrate concentrations as a function of r are:

$$\frac{\mathrm{d}^2[\mathrm{AcD}]}{\mathrm{d}r^2} + \frac{2}{r}\frac{\mathrm{d}[\mathrm{AcD}]}{\mathrm{d}r} - \frac{1}{D_{\mathrm{Aeff}}} \times \frac{\left(k_{\mathrm{Synth}}[\mathrm{Nuc}] + k_{\mathrm{Hydr}}\right)[\mathrm{AcD}][E_0]}{K_{\mathrm{N}} + [\mathrm{Nuc}]} = 0 \tag{7}$$

$$\frac{\mathrm{d}^2[\mathrm{Nuc}]}{\mathrm{d}r^2} + \frac{2}{r}\frac{\mathrm{d}[\mathrm{Nuc}]}{\mathrm{d}r} - \frac{1}{D_{\mathrm{Neff}}}\frac{k_{\mathrm{Synth}}[\mathrm{Nuc}][\mathrm{AcD}][E_0]}{K_{\mathrm{N}} + [\mathrm{Nuc}]} = 0 \tag{8}$$

An equivalent system involving only first-order differential equations is:

$$\frac{\mathrm{dDA}}{\mathrm{d}r} + \frac{2}{r}\mathrm{DA} - \frac{1}{D_{\mathrm{Aeff}}} \times \frac{\left(k_{\mathrm{Synth}}[\mathrm{Nuc}] + k_{\mathrm{Hydr}}\right)[\mathrm{AcD}][E_0]}{K_{\mathrm{N}} + [\mathrm{Nuc}]} = 0 \tag{9}$$

$$\mathrm{DA} = \frac{\mathrm{d}[\mathrm{AcD}]}{\mathrm{d}r} \tag{10}$$

$$\frac{\mathrm{dDN}}{\mathrm{d}r} + \frac{2}{r}\mathrm{DN} - \frac{1}{D_{\mathrm{Neff}}}\frac{k_{\mathrm{Synth}}[\mathrm{AcD}][\mathrm{Nuc}][E_0]}{K_{\mathrm{N}} + [\mathrm{Nuc}]} = 0 \tag{11}$$

$$\mathrm{DN} = \frac{\mathrm{d}[\mathrm{Nuc}]}{\mathrm{d}r} \tag{12}$$

These equations, subjected to the boundary conditions:

$$r = 0 \Rightarrow \begin{cases} \mathrm{DA} = 0 \\ \mathrm{DN} = 0 \end{cases} \text{ and } r = R \Rightarrow \begin{cases} [\mathrm{AcD}] = [\mathrm{AcD}]_{\mathrm{B}} \\ [\mathrm{Nuc}] = [\mathrm{Nuc}]_{\mathrm{B}} \end{cases} \tag{13}$$

yield as a solution the concentration profiles of substrates as functions of r inside the porous biocat-

alyst particles. The initial rate of consumption of each of the substrates by unit of mass of biocatalyst is given by the rate of transfer across the outer surface of the particles divided by the mass of a particle:

$$\text{Rate}_A = \frac{4\pi R^2}{M_P} D_{Aeff} \left.\frac{d[AcD]}{dr}\right|_{r=R} \quad (14)$$

and

$$\text{Rate}_N = \frac{4\pi R^2}{M_P} D_{Neff} \left.\frac{d[Nuc]}{dr}\right|_{r=R} \quad (15)$$

The apparent initial rate of peptide synthesis is given by Rate_N, since the nucleophile is only consumed for peptide synthesis, while the apparent nucleophile selectivity, defined by the ratio of peptide synthesis to acyl donor hydrolysis, is given by $(\text{Rate}_N/\text{Rate}_A - \text{Rate}_N)$, since the acyl donor is both used for peptide synthesis and hydrolyzed.

Given the nonlinear nature of the intrinsic enzyme kinetics, the differential equations have to be solved numerically. However, numerical methods can only solve initial value problems, which imply that the concentrations of substrates at the centre of the particles are known. Since this is not the case, an iterative method was used that performed the following steps:

1. Assumption of initial values of the concentrations of substrates at the center of the particle.
2. Resolution of the differential equations by a numeric procedure.
3. Comparison of the concentrations of substrates calculated for the surface of the particle with the respective concentrations on the bulk solution.
4. If needed, correction of the initial values of the concentrations at the center of the particle, multiplying by the ratio of bulk solution concentration to calculated concentration at the surface.
5. Repetition of steps 2 to 4, until the relative differences between bulk solution concentration and calculated concentration at the surface of the particle for both substrates are less than a predefined tolerance value.

This routine was implemented in MATLAB language, using the software package MATLAB 4.2c for Macintosh, ©1984–94 The MathWorks, and the respective function ODE45, which integrates the differential equation system using the fourth and fifth order Runge–Kutta formulas. The initial values assumed for the substrate concentrations at the centre of the biocatalyst particles were the same as the bulk solution concentrations (20 mM for acyl donor and 30 mM for nucleophile), and the allowed tolerance value for the relative concentration differences was 10^{-5}.

In order to take into account the particle size distribution of each support material, the range of particle sizes was divided into 12 subranges and the differential equations calculations were carried out for each of the 12 subrange average values of particle size. The results for each support material were the weighted averages obtained with the results of each subrange. This treatment proved to be relevant only for the calculations with celite, which has a bimodal particle size distribution with particle diameter maxima around 20 and 200 μm [25]. With the polyamide materials, the results obtained using the particle size distribution approximation agreed well with those obtained using the average particle size diameter.

3. Experimental

3.1. Chemicals

Bovine pancreas α-chymotrypsin (CT, Specific activity 52 BTEE U mg solid^{-1}) and triethylamine (TEA) were purchased from Sigma, USA. *N*-acetyl-L-phenylalanine ethyl ester (AcPheOEt), *N*-benzoyl-L-tyrosine ethyl ester (BzTyrOEt), *N*-benzoyl-L-alanine methyl ester (BzAlaOMe), L-alaninamide hydrochloride (AlaNH_2.HCl) and L-alanyl-L-phenylalaninamide hydrochloride (AlaPheNH_2.HCl) were purchased

Table 2
Physical characteristics of the support materials used

Support material	Average R (μm)	P ($cm^3\ g^{-1}$)	ρ ($g\ cm^{-3}$)
PAm 300–500	248	0.56	0.74
PAm 106–180	89	0.56	0.74
Celite	73	0.06	1.45

from Bachem Feinchemikalien, Switzerland. Acetonitrile (HPLC grade), glacial acetic acid and tris(hydroxymethyl)-aminomethane (Tris) were from Merck, Germany.

3.2. Supports

Celite and polyamide supports of two particle size ranges, PAm 106–180, with mean particle diameter 178 μm, and PAm 300–500, with mean particle diameter 495 μm, were prepared as previously reported [25]. Determinations of specific surface area, area distribution with pore diameter, porosity, skeletal density, pore size distribution and particle size distribution were performed on these granular materials, and the results have been published [25]. Table 2 resumes the most relevant physical characteristics of these materials.

3.3. Initial rate and nucleophile selectivity measurements

The following combinations of acyl donors and nucleophiles were used: BzAlaOMe + $AlaNH_2$; AcPheOEt + $AlaNH_2$; BzTyrOEt + $AlaNH_2$ and BzTyrOEt + $AlaPheNH_2$. The experimental initial rates and nucleophile selectivities obtained using immobilized α-chymotrypsin on the studied supports were obtained as previously reported [11,21].

The intrinsic kinetic measurements that have been previously carried out by employing thin immobilized enzyme layers on nonporous glass beads [22] with some of these reactions were extended to the tripeptide synthesis reaction BzTyrOEt + $AlaPheNH_2$ in order to estimate k_{Synth}, k_{Hydr} and K_N. The results for this reaction agreed well with Eqs. (3) and (4). The estimated kinetic parameters, intrinsic rates and nucleophile selectivities for all these reactions are presented in Table 3.

4. Results and discussion

4.1. Concentration profiles

Typical concentration profiles obtained by solving the differential Eqs. (9)–(12) are shown in Fig. 1. As the enzyme loading increases, the concentration gradients become steeper for both acyl donor and nucleophile which is an indication of stronger mass transfer limitations, as expected. In the case of 30 mg/g loading, practically no reactions occur on the inner 50 μm core of celite particles with 73 μm radius. It can be seen that in all cases the concentration gradients are more steep for the acyl donor than for the nucleophile. This is mainly due to the higher diffu-

Table 3
Intrinsic kinetic parameters for the reactions studied

Reaction	k_{Synth} ($ml\ min^{-1}\ g\ CT^{-1}$)	k_{Hydr} ($\mu mol\ min^{-1}\ g\ CT^{-1}$)	K_N (mM)	Nucleophile selectivity[a]	Intrinsic rate[a] ($\mu mol\ min^{-1}\ g\ support^{-1}$)
BzAlaOMe + $AlaNH_2$	0.86	1.7	11.0	15.2	1.14
AcPheOEt + $AlaNH_2$	35	54	9.8	19.4	48
BzTyrOEt + $AlaNH_2$	420	580	6.0	21.7	640
BzTyrOEt + $PheAlaNH_2$	82	430	3.9	5.2	132

[a]Calculated from the intrinsic kinetic parameters for a preparation containing 100 mg enzyme per gram support material and bulk substrate concentrations of 20 mM acyl donor and 30 mM nucleophile in the absence of mass transfer limitations.

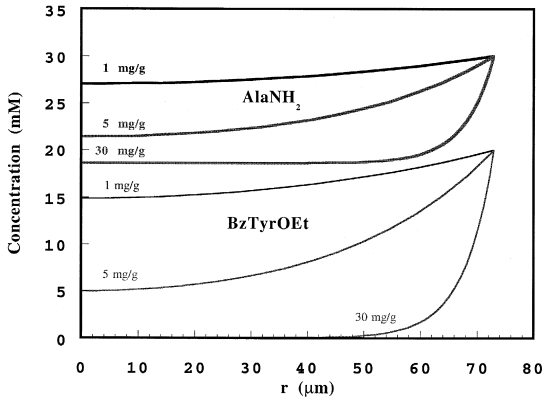

Fig. 1. Calculated concentration profiles on celite particles with $r = 73$ μm, for the substrate combination BzTyrOEt + $AlaNH_2$. Thick lines — nucleophile concentrations; thin lines — acyl donor concentrations. The assumed enzyme loading is indicated by the labels next to the lines.

sion coefficient for the nucleophilic substrate (cf. Table 1), and also to a smaller extent due to the larger consumption of acyl donor, which participates in both synthetic and hydrolytic reactions (1) and (2), while the nucleophile only participates in the synthetic reaction (1). Also, the residual concentration of nucleophile at the center of the particles is always much higher than the acyl donor concentration. This is because besides the lower gradient inside the biocatalyst particles, the concentration of nucleophile is also larger in the bulk solution. As a conclusion, mass transfer limitations have a stronger effect on the acyl donor than on the nucleophilic substrate.

4.2. Model *vs.* experimental results

The assumed pore tortuosity values that gave a better agreement between model calculations and experimental results were 8 for celite and 12 for the polyamides. These are close to the ranges of values cited in the literature: Bailey and Ollis [27] state that this parameter ranges between 1.4 and 7 for most porous materials, while Smith [24] mentions a range from under unity (with surface diffusion) up to 6, suggesting a value of 4 in the absence of other data. Even though the values used here are just outside these ranges, one should bear in mind also that the estimation of the bulk solution diffusion coefficients was only roughly made through theoretical correlations that try to take into account the natures of both the solvent and the diffusing molecules, which is quite an ambitious task. Since the diffusion coefficients and the tortuosity values are combined to calculate the effective diffusion coefficients through Eq. 6, assuming higher tortuosities is equivalent to assuming lower diffusion coefficients by the same factor.

4.3. Effect of the support material

Fig. 2 compares, for one of the reactions modeled, the experimental and model calculated profiles of the experimental rates and nucleophile selectivities with variation of the support material. The agreement between model and experiments is reasonable, even though the model overestimates the initial rates on PAm 300–500 at high enzyme loadings. It is, however, important to notice that the model accurately predicts the lowering of the initial rate with increased enzyme loading when celite is used as support, an odd experimental observation that has been conceptually explained before [11] and here finds a sturdy numeric support. As previously reported, the cause of this lowering in initial rate is the increased

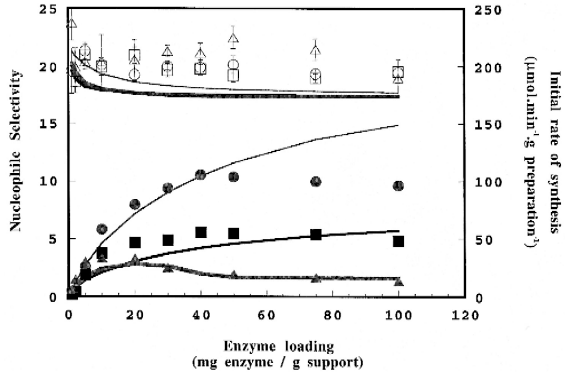

Fig. 2. Experimental observations (symbols) and model predictions (lines) for initial rate (closed symbols) and nucleophile selectivity (open symbols) of the dipeptide synthesis reaction BzTyrOEt + $AlaNH_2$ with variation of the support material: PAm 106–180 (circles and thin lines), PAm 300–500 (squares and normal lines) and celite (triangles and thick lines)

proportion of the pore space of celite that is occupied by insoluble enzyme molecules, leaving very little room for substrate diffusion (cf. Eq. 6). Also important to notice is that the onset of mass-transfer limitations has a much more important effect on limiting the initial rates than on reducing nucleophile selectivity. In agreement with the experimental observations, the model predicts little change of this last parameter with enzyme loading or with support material. Since from the kinetic point of view nucleophile selectivity depends only on the concentration of nucleophile (Eq. 5), this small effect of mass-transfer limitations is justified by the relatively small nucleophile concentration gradients that are expected to exist inside the biocatalyst particles, as seen in Fig. 1.

Clearly, the model correctly incorporates the nature of the support material, yielding results that agree satisfactorily with the experimental observations.

4.4. Effect of the nature of the reaction

Fig. 3 compares, using celite as the support material, the experimental and model calculated profiles of the initial rate and nucleophile selectivities, using two other acyl donors: BzAlaOMe (Fig. 3A) and AcPheOEt (Fig. 3B). Also in these cases, the numeric agreement between the model calculations and experiments is reasonable. For these reactions, the plateau-shaped initial rate profiles are also predicted by the model calculations, their main cause being the impossibility of accommodating all the enzyme molecules on the support at high loadings. Also in these cases, the model predicts only limited reduction of nucleophile selectivity with enzyme loading. The scattering of the nucleophile selectivity experimental data obtained for these reactions is explained by two different reasons: the low rates of the reactions involving BzAlaOMe as acyl donor, and the low sensitivity of the HPLC analyses performed with AcPheOEt as acyl donor — unlike in all other cases, this molecule lacks the benzoyl N-protecting group, which is responsible for a very strong UV absorption. Given these limitations in the collection of the experimental data, the agreement between the model and experiments can be considered reasonable.

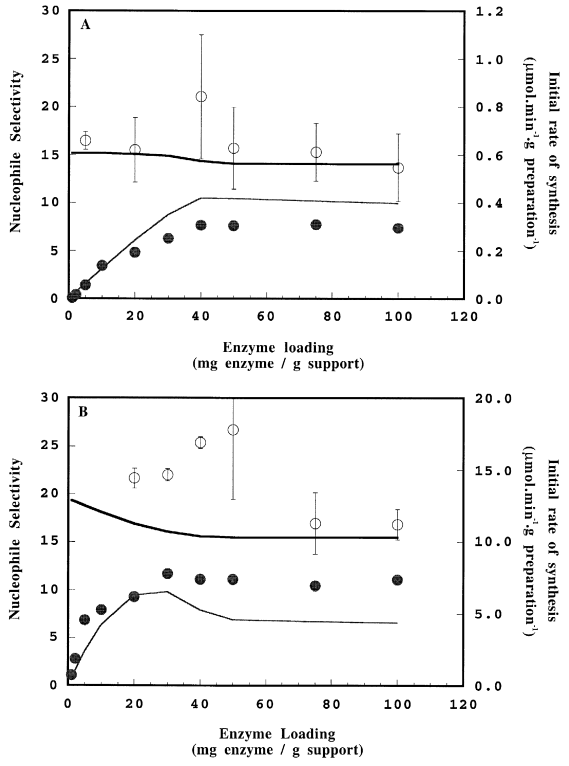

Fig. 3. Experimental observations (symbols) and model predictions (lines) for initial rate (closed circles and thin lines) and nucleophile selectivity (open circles and thick lines) with enzyme immobilized on celite and $AlaNH_2$ as nucleophile as with variation of the acyl donor: BzAlaOMe (A) or AcPheOEt (B). Compare with Fig. 2 for the case of BzTyrOEt.

Fig. 4 compares the nucleophile selectivity profiles when two different nucleophiles, $AlaNH_2$ and $AlaPheNH_2$, are used with BzTyrOEt as acyl donor and PAm 300–500 as support material. The model predicts a larger decrease of nucleophile selectivity with enzyme loading when the bulkier nucleophile is used, which agrees with the experimental observations. The reasoning is that the diffusional transport of the bulkier nucleophile, with a lower diffusion coefficient, will need steeper gradients inside the biocatalyst particles, and in this way the effect on nucleophile selectivity is larger. The experimentally observed difference between the two nucleophiles is larger than what is predicted by the model. The agreement between model and experiments can be increased by adjusting the estimation of the diffusion

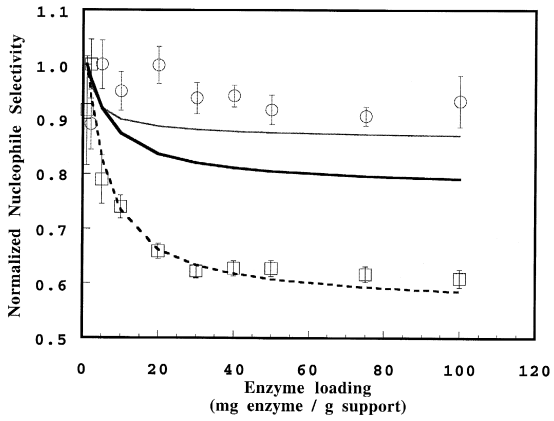

Fig. 4. Experimental observations (symbols) and model predictions (lines) for normalized nucleophile selectivity with enzyme immobilized on PAm 300–500 and BzTyrOEt as acyl donor with variation of the nucleophile: $AlaNH_2$ (circles and thin line) or $AlaPheNH_2$ (squares, thick and dashed lines). To obtain the dashed line, the diffusion coefficient of $AlaPheNH_2$ listed in Table 1 was divided by 2. The values of nucleophile selectivities corresponding to the normalized value of 1.0 are those listed in Table 3.

coefficient of the bulkier nucleophile. If the value of the diffusion coefficient of $AlaPheNH_2$ listed in Table 1 is divided by 2, the dashed line in Fig. 4 represents the model calculations, which agree better with experimental results.

The model then correctly incorporates the information specific for different reactions — intrinsic kinetics and diffusion coefficients — in order to produce realistic estimates of the initial rate and nucleophile selectivity profiles. In the case of the initial rates, the experimentally observed values range three orders of magnitude, but the model is still able to predict them satisfactorily, which indicates a broad range of successful estimation conditions.

5. Conclusions

The model built for two-substrate, simultaneous diffusion and two-reaction kinetics inside the porous biocatalyst particles numerically predicts the apparent initial rate and enzyme selectivity vs. the loading profiles with a reasonable agreement with the experimental observations. Both the effect of the support material and the nature of the catalyzed reaction are correctly predicted by the numeric calculations, even though the experimental observations range three orders of magnitude in the case of the initial rates. The model predicts a larger effect of mass-transfer limitations on the initial rates than on the nucleophile selectivity of kinetically controlled peptide synthesis reactions, and is accurate at predicting a reduction in the initial rate with increased enzyme loading with certain non-porous support materials, a surprising experimental observation previously reported [11, 28]. This model gives a sound numerical support to the conceptual explanation then presented in terms of reduced space for substrate diffusion [11].

The main limitation with the present model is the estimation of the effective diffusion coefficients of the substrates. In their calculation, the pore tortuosity was given arbitrary values for each support that leads to good agreement with the experimental data, and the bulk solution diffusion coefficients were estimated by the theoretical correlations that might be subjected to large uncertainties. In some cases, it is possible to measure experimentally the effective diffusion coefficients [24], but that involves the availability of the porous material as a membrane or a slab through which the rate of transport of the substrates can be measured. This was not the case for the materials used in this study.

In this particular study, kinetically controlled peptide synthesis reactions catalyzed by α-chymotrypsin were modeled, but if kinetic, diffusional, support and enzyme parameters characteristic for other situations are fed into the model, other reactions and experimental conditions can be simulated. In this way, the model is a general tool that allows prediction of the relative importance of mass transfer limitations, which can help to optimize the conceptual design of a biotransformation process.

6. Nomenclature

[AcD]	Concentration of acyl donor (mM)
$[E_0]$	Amount of enzyme (mg ml^{-1})
[HyP]	Concentration of hydrolysis product, mM
[Nuc]	Concentration of nucleophile, mM
[Pep]	Concentration of peptide product, mM

AcPheOEt	*N*-acetyl-L-phenylalanine ethyl ester
AlaNH2	L-alaninamide
AlaPheNH2	L-alanyl-L-phenylalaninamide
BzAlaOMe	*N*-benzoyl-L-alanine methyl ester
BzTyrOEt	*N*-benzoyl-L-tyrosine ethyl ester
D	Diffusion coefficient ($cm^2\ s^{-1}$)
k_{Hydr}	Kinetic constant ($\mu mol\ min^{-1}\ mg\ CT^{-1}$)
K_N	Kinetic constant (mM)
k_{Synth}	Kinetic constant ($ml\ min^{-1}\ mg\ CT^{-1}$)
LG	Leaving group (ethanol or methanol)
M_P	Mass of a biocatalyst particle
P	Particle porosity ($cm^3\ g^{-1}$)
r	distance from the centre of the particle
R	Particle radius
t	time
ε	Volumetric porosity
ρ	Particle density ($g\ cm^{-3}$)
τ	Pore tortuosity
Subscripts	
A	Acyl donor
B	Bulk solution
eff	effective
N	Nucleophile

Acknowledgements

This work was financially supported by the Portuguese Foundation for Science and Technology (FCT, MCT) through the grant BD/2839/94 of the program PRAXIS XXI and the Swedish Research Council for Engineering Sciences (TFR).

References

[1] V.M. Paradkar, J.S. Dordick, J. Am. Chem. Soc. 116 (1994) 5009.
[2] G. Bell, P.J. Halling, B.D. Moore, J. Partridge, D.G. Rees, Trends Biotechnol. 13 (1995) 468.
[3] P. Adlercreutz, in: A.M.P. Koskinen, A.M. Klibanov (Eds.), Enzymatic Reactions in Organic Media, Chapman & Hall, Glasgow, UK, 1996, p. 9, Chap. 2.
[4] Z. Yang, A.J. Russell, in: A.M.P. Koskinen, A.M. Klibanov (Eds.), Enzymatic Reactions in Organic Media, Chapman & Hall, Glasgow, UK, 1996, p. 43, Chap. 3.
[5] A.M. Klibanov, Trends Biotechnol. 15 (1997) 97.
[6] A. Rosevear, J. Chem. Tech. Biotechnol. 34B (1984) 127.
[7] J.S. Dordick, Enzyme Microb. Technol. 11 (1989) 194.
[8] W. Tischer, V. Kasche, Trends Biotechnol. 17 (1999) 326.
[9] T. Kiesser, G.A. Oertzen, W. Bauer, Chem. Eng. Technol. 13 (1990) 80.
[10] S. Kamat, E.J. Beckman, A.J. Russell, Enzyme Microb. Technol. 14 (1992) 265.
[11] R.J. Barros, E. Wehtje, P. Adlercreutz, Biotechnol. Bioeng. 59 (1998) 364.
[12] D. Vasic-Racki, M. Gjumbir, Bioproc. Eng. 2 (1987) 59.
[13] A.V. Gusakov, Biocatalysis 1 (1988) 301.
[14] S. Guzy, G.M. Saidel, N. Lotan, Bioproc. Eng. 4 (1989) 239.
[15] V.K. Jayaraman, Biotechnol. Lett. 13 (1991) 455.
[16] S. Zvirblis, E. Dagys, A. Pauliukonis, Biocatalysis 6 (1992) 247.
[17] P. Bernard, D. Barth, Biocatal. Biotransform. 12 (1995) 299.
[18] S. Sato, T. Murakata, T. Suzuki, M. Chiba, Y. Goto, J. Chem. Eng. Jpn. 30 (1997) 654.
[19] B.A. Bedell, V.V. Mozhaev, D.S. Clark, J.S. Dordick, Biotechnol. Bioeng. 58 (1998) 654.
[20] H.J. Vos, P.J. Heederik, J.J.M. Potters, K.Ch.A.M. Luyben, Bioproc. Eng. 5 (1990) 63.
[21] R.J. Barros, E. Wehtje, P. Adlecreutz, Biotechnol. Bioeng. 67 (2000) 319.
[22] R.J. Barros, A. Paar, E. Wehtje, P. Adlercreutz, Ann. N.Y. Acad. Sci. 864 (1998) 188.
[23] R.C. Reid, J.M. Prausnitz, B.E. Poling, The Properties of Gases and Liquids, 4th edn., McGraw-Hill, New York, USA, 1987.
[24] J.M. Smith, Chemical Engineering Kinetics, 3rd edn., McGraw-Hill, New York, USA, 1981.
[25] R.J. Barros, E. Wehtje, F.A.P. Garcia, P. Adlercreutz, Biocatal. Biotransform. 16 (1998) 67.
[26] L. Stryer, Biochemistry, 3rd edn., Freeman, New York, USA, 1988.
[27] J.E. Bailey, D.F. Ollis, Biochemical Engineering Fundamentals, 2nd edn., McGraw-Hill, New York, USA, 1986.
[28] M. Capellas, M.D. Benaiges, G. Caminal, G. González, J. López-Santín, Biocatal. Biotransform. 13 (1996) 165.